Am J Cancer Res 2022;12(7):3437-3454
www.ajcr.us /ISSN:2156-6976/ajcr0143106

Original Article

Overexpression of glucocorticoid receptor promotes the poor progression and induces cisplatin resistance through p38 MAP kinase in cervical cancer patients

Gwan Hee Han[1], Hee Yun[2], Julie Kim[3], Joon-Yong Chung[4], Jae-Hoon Kim[5,6], Hanbyoul Cho[5,6]

[1]Department of Obstetrics and Gynecology, Kyung Hee University Hospital at Gangdong, Seoul 05278, Republic of Korea; [2]Department of Obstetrics and Gynecology, Gangnam Severance Hospital, Yonsei University College of Medicine, Seoul 06299, Republic of Korea; [3]Weill Cornell Medical College, 1300 York Ave, New York, NY 10065, USA; [4]Molecular Imaging Branch, Center for Cancer Research, National Cancer Institute, National Institutes of Health, Bethesda, MD 20892, USA; [5]Department of Obstetrics and Gynecology, Yonsei University College of Medicine, Seoul 06299, Republic of Korea; [6]Institute of Women's Life Medical Science, Yonsei University College of Medicine, Seoul 03722, Republic of Korea

Received March 25, 2022; Accepted June 20, 2022; Epub July 15, 2022; Published July 30, 2022

Abstract: Glucocorticoid receptor (GR) is activated by synthetic glucocorticoid or endogenous cortisol which were released by the physical and psychosocial stress, and recent studies reported that it is involved in tumor initiation and metastasis in various solid cancers. However, role of GR in cervical cancer has not been elucidated yet. Therefore, here we aim to unveil the role of GR in cervical cancer with cervical cancer clinical specimen and cervical cancer cell lines. We found that overexpression of GR was associated with poor prognosis in cervical cancer patients. Also, GR knockdown in cervical cancer cell lines showed diminished proliferation, invasion and EMT properties. Besides, we found that GR was positively associated with FoxP3 expression, and combination of GR and FoxP3 overexpression revealed as more reliable biomarker for poor prognosis and poor response to chemotherapy of cervical cancer patient than GR alone. Moreover, FACS-based Annexin-V/PI double staining and cleavage of poly ADP ribose polymerase (PARP) showed that siGR enhanced cisplatin-induced apoptosis, which was mediated by p38 MAP kinase. Collectively, our findings established that the combination of high GR and FoxP3 was associated with cervical cancer progression and platinum resistance, suggesting a potential predictive biomarker for clinical management in patients with cervical cancer.

Keywords: Glucocorticoid receptor, FoxP3, cervical cancer, cisplatin resistance, biomarker

Introduction

Cervical cancer which showed 341,831 disease related mortality in year 2020 worldwidely, represents the fourth most deadly malignancy in women. Also, 604,127 new cases in 2020 of cervical cancer has been reported [1]. During the past few decades, the overall mortality and incidence rate of cervical cancer have declined owing to the development of cervical cancer screening and a powerful preventative vaccine [2, 3]. However, patients diagnosed with advanced-stage or recurrent cervical cancers have been frequently observed to have an exceedingly low survival rate. Thus, it is urgent to investigate biomarkers to unveil the mechanisms related to cervical cancer progression mechanisms and predict the prognosis of cervical cancer. The glucocorticoid receptor (GR), nuclear hormone receptor, is activated by synthetic glucocorticoid or endogenous cortisol, which regulates the transcription of hundreds of genes depending on the state of physical and psychosocial stresses [4, 5]. Several lines of evidence suggest that such physical and psychosocial stresses provoke the disruption of the neuroendocrine axis, which may be related to the increased onset, progression, and mortality of cancer. In addition, GR-mediated signaling pathway has been demonstrated to reduce the anti-cancer effect of chemotherapy in cell lines and xenograft models by inhibiting apop-

tosis in breast [6, 7], pancreatic [8] and epithelial ovarian cancer (EOC) [9-12].

FoxP3, a transcription factor which to be a member of Foxhead box (FOX) protein, was first found master regulator modulating the function and development of immune suppressive T regulatory cells (Tregs), and has been linked to various diseases including autoimmune diseases or allergic reactions [13]. In addition, recent studies have revealed that FoxP3 overexpression is closely related to poor prognosis and facilitates distant metastasis by inhibiting the immune response in patients with various types of cancers such as EOC [14, 15], oral squamous cell carcinoma [16], and breast cancer [17-19]. In cervical cancer, a previous report demonstrated that FoxP3 may promote proliferation and invasion, and reduce apoptosis, thereby enhancing malignancy [20]. However, the underlying mechanisms that affect endogenous tumor-specific immunity and pathogenesis are still unclear.

Here, we object to verify the expression level of GR and its underlying molecular mechanism in cervical cancer clinical specimen and cervical cancer cell lines. In addition, effect of GR in expression of FoxP3 has been reported from previous studies, we objected to assess the correlation between GR and FoxP3 in cervical cancer.

Material and methods

Collection of specimens and clinicopathological characteristics

Three hundred non-adjacent normal cervical epithelial tissues, 310 cervical intraepithelial neoplasias (CINs; 102 low grade CINs and 218 high grade CINs) and 188 cervical cancer tissues obtained from the patients included in this study. They were operated on either type 3 radical hysterectomy with pelvic lymph node (LN) dissection or conization at the Department of Obstetrics and Gynecology, Gangnam Severance Hospital, Yonsei University College of Medicine between March 1996 and March 2010, and some formalin-fixed, paraffin-embedded (FFPE) blocks were donated by the Korea Gynecologic Cancer Bank under the Bio & Medical Technology Development Program of the Ministry of the National Research Foundation (NRF), which was funded by the Korean government (MIST) (NRF-2017M3A9B80696-10). All adequate specimens which were reviewed by pathologists were included in this study. The clinicopathological characteristics of the specimen used in the study, including age, cell type, tumor size, LN metastasis, tumor grade, or involvement of lymphovascular space invasion (LVIS), survival time, survival status, and concurrent chemoradiation therapy (CCRT) response were gathered from medical and pathology records. Cervical cancer staging and grading of tumor were done based on 2018 The International Federation of Gynecology and Obstetrics (FIGO) staging system, and World Health Organization (WHO) grading system [21]. After surgical resection, patients who were at high risk of relapse, such as those with positive LNs, positive resection margins, or parametrial invasion by pathology report underwent CCRT. The response evaluation criteria in solid tumors (RECIST; version 1.1) with either by magnetic resonance imaging (MRI) or computed tomography (CT) was adapted to evaluate the overall response of therapy (21). The study was approved by Institutional Review Board (IRB) of Gangnam Severance Hospital (IRB no. 3-2020-0377).

Tissue microarray construction and immunohistochemistry analysis

Tissue microarrays (TMAs) used in this study were constructed as described previously (22). For immunohistochemistry (IHC). TMAs were dissected as 5 μm thick serially, and underwent deparaffinization and rehydration with xylene, serially graded ethanol, and distilled water. Respectively, afterwards, 3% hydrogen peroxide (H_2O_2) was applied for 10 min to block the endogenous peroxidase. For antigen retriever, the slides were placed in steam pressure cooker (Pascal; Dako, Carpinteria, CA) with preheated buffer of pH 6 (Dako) for 20 min. Next, the primary antibodies, an anti-GR antibody (rabbit antibody, clone #3660S, 1:400; Cell Signaling Technology, Danvers, MA) and anti-FoxP3 antibody (mouse antibody, clone #14-4777-82, 1:300; eBioscience, San Diego, CA), were treated for 1 hr in Dako Autostainer Plus (Dako) after inhibiting nonspecific staining for 10 min with a protein block (Dako). Then, the Dako EnVision+Dual Link System-HRP (Dako) and 3,3-diaminobenzidine (DAB; Dako) were used to color the sections and for antigen-antibody

reaction. Finally, hematoxylin was used to counterstain the slides and they were mounted. Finally, the slides were examined under a light microscope.

Evaluation of IHC staining

After IHC staining, the stained slides were scanned with the Nanozoomer 2.0 HT (Hamamatsu Photonics K.K., Hamamatsu City, Japan). Then, the automatic digital image analysis software, Visiopharm Integrator System v6.5.0.2303 (VIS; Visiopharm, Hørsholm, Denmark) was used to score the percentage and intensity of positively stained GR or FoxP3 in clinical specimens after appropriate training of the program. The scoring was categorized as 0: negative, 1: weak, 2: moderate, and 3: strong for staining intensity. The histoscore was calculated by multiplying the intensity of target genes and percentage (0-100) of positive cells without any clinical data.

Tumor Immune Estimation Resource 2.0 (TIMER 2.0)

The Tumor Immune Estimation Resource 2.0 (TIMER 2.0, http://timer.comp-genomics.org/) [22], a tool used to analyze immune cell infiltration in various tumors, was used to study whether the expression of GR is related to immune infiltration and FoxP3 in cervical cancer.

Cell culture and reagents

Caski and SiHa human cervical cancer cell lines were commercially purchased from the Korea Cell Line Bank (Seoul, Republic of Korea). All cell lines were grown in RPMI 1640 supplemented with 10% fetal bovine serum (FBS), 1% streptomycin, and 1% penicillin. Also, they were incubated at 37°C with 5% CO_2 containing humidified atmosphere. Dexamethasone and SB203582 was obtained from Sigma-Aldrich (St. Louis, MO) and Selleck Chemicals (Houston, TX).

siRNA transfection

GR and FoxP3 targeting specific small interfering RNAs (siRNAs) were commercially purchased from Santa Cruz Biotechnology (Santa Cruz, CA). siRNA was transfected into 6-wells plates using Lipofectamine® RNAiMAX Reagent (Invitrogen, Gaithersburg, MD) at a dose of 50 pmol per well according to the manufacturer's instructions.

Western blotting analysis

Cell lysates were extracted with cell lysis buffer (Cell Signaling Technology) containing PMSF and SDS-PAGE was used to resolve the proteins from the cell lysates and transferred to nitrocellulose membrane. Antibodies against GR, FoxP3, and β-actin were purchased from Santa Cruz Biotechnology (Santa Cruz), and antibodies against PARP, phospho-$p38^{Thr180/Tyr182}$, p38, Slug, and E-cadherin were purchased from Cell Signaling Technology. Enhanced chemiluminescence reagents (Thermo Fisher Scientific, Waltham, MA) were used to visualize the immunoreactive bands.

Flow cytometric analysis

After treating Caski and SiHa cells with cisplatin, they were treated with Annexin V-FITC (BD Biosciences, Waltham, MA) and propidium iodide (PI) in a dark at room temperature for 15 min to evaluate the apoptosis. Then, the binding buffer was used to dilute the stained cells and flow cytometry was used to analyze. Flow cytometric analyses were completed on a FACS-Canto II analyzer (BD Biosciences), and FACSDiva software (BD Biosciences).

Boyden chamber assay

The 48-well microchemotaxis chambers (Neuro Probe, Gaithersburg, MD) containing culture medium with 10% FBS in the bottom chamber of each well were applied for cell invasion examination. The membranes (#PFB8; Neuro Probe) which were immersed with Matrigel (BD Biosciences) were placed over the bottom chamber walls After 48 hr seeding siRNA-transfected cells (1×10^5 cells/50 μL of medium containing 0.05% FBS) in the upper chambers, the uninvaded cells were wiped out from the upper surface of the membrane, a Diff-Quick solution (Sysmex, Kobe, Japan) was used to stain and fix the membrane. The invading cells were counted in six random high-power fields per filter (HPF) using an Axio Imager M2 microscope (Carl Zeiss, Thornwood, NY). The experiments were repeated at least three times.

Real-time quantitative RT-PCR

The AccuPrep® Universal RNA Extraction Kit (Bioneer, Seoul, Republic of Korea) was used to isolate the total RNA, and AccuPower® RocketScript™ RT PreMix (Bioneer) was used to construct cDNA as manufacturers recommended. Real-time quantitative PCR was done with TOPrealTM qPCR 2X PreMIX (SYBR Green with high ROX; Enzynomics, Daejeon, Republic of Korea) on an Applied Biosystems 7300 real-time PCR system (Applied Biosystems, Foster City, CA). The reaction conditions were as follows: pre-incubation at 94°C for 10 min, with 40 cycles of 94°C for 10 sec, 60°C for 15 sec, 72°C for 15 sec, and a melting curve program by programing the temperature to rise from 60°C to 95°C. To calculate relative mRNA expression levels, the comparative cycle threshold ($2^{-\Delta\Delta Ct}$) method was used, and the β-actin gene was used as the endogenous control for normalization. Primers were purchased from Bioneer: FoxP3 5-CCTACCCACTGCTGGCAAA-3 (forward); 5-CCTGGCAGTGCTTGAGGAA-3 (reverse); GAPDH 5-AGAAGGCTGGGGCTCATTTG-3 (forward), and 5-AGGGGCCATCCACAGTCTTC-3 (reverse). Each experiment was repeated at least three times.

Cell proliferation assay

To test cell proliferation, the EZ-Cytox assay kit (Daeil Lab Service, Seoul, Republic of Korea) was use as the manufacturer's recommended. To measure the absorbance, the microplate reader (Bio-Rad Laboratories, Inc., Hercules, CA) at 450 nm was used in each well. Each experiment was performed in at least three times.

Colony formation assay

siRNA of FoxP3 with Caski and SiHa cells were transfected for 24 hr. After 24 hr, the cells (500 cells/well) were placed in a 6-well plate and placed for 2 weeks in an incubator at 37°C with 5% CO_2. Then, the cells were fixed for 10 mins with methanol and stained with 0.5% crystal violet for 30 min. respectively. After washing with distilled water, the colony formation was countered by a microscope, and each experiment was performed at least in triplicates.

Statistical analysis

The Mann-Whitney test, Kruskal-Wallis test, or Pearson Chi-square test were used for GR or FoxP3 expression statistical analysis when appropriate. To estimate disease-free survival (DFS) and overall survival (OS), the Kaplan-Meier method was used, and the log-rank test was performed to compare the two groups. The Cox proportional hazard model was performed to evaluate hazard ratios (HRs) and confidence intervals (CIs) for univariate and multivariate models. The Spearman's rank correlation method was used to evaluate the correlation between GR and FoxP3. Statistical analyses were performed using either SPSS (version 23.0, SPSS Inc., Chicago, IL) or R 3.32 (Vienna, Austria; http://www.R-project.org). The probability (*p*) values less than 0.05 were set statistically significant.

Results

GR or FoxP3 protein expression in cervical cancer

First, to determine the clinical relevance of GR or FoxP3 expression in cervical cancer, we performed IHC in cervical cancer tissues, CINs, and non-adjacent normal cervical epithelia, and representative IHC images are shown in **Figure 1A**. GR expression was observed in the nucleus and was overexpressed in the cervical cancers and CINs compared to in the nonadjacent normal cervical epithelial. Also, GR expression was higher in FIGO stage II-IV than FIGO stage I ($P < 0.001$; **Figure 1B** and **Table 1**) and associated with poor CCRT response ($P = 0.041$; **Table 1**). For FoxP3, it was significantly overexpressed in cervical cancer tissues than in precursor lesions, and non-adjacent normal cervical epithelial ($P < 0.001$ **Figure 1B** and **Table 1**) and was related to FIGO stage II-IV ($P = 0.041$; **Figure 1B** and **Table 1**). In short, these results indicate that GR and FoxP3 expression would be invaluable biomarkers to predict progression of cervical cancer.

Prognostic significance of GR and FoxP3 expression and correlation between GR and FoxP3 in cervical cancer specimen

Next, we evaluated the prognostic value of GR or FoxP3 expression in patients with cervical

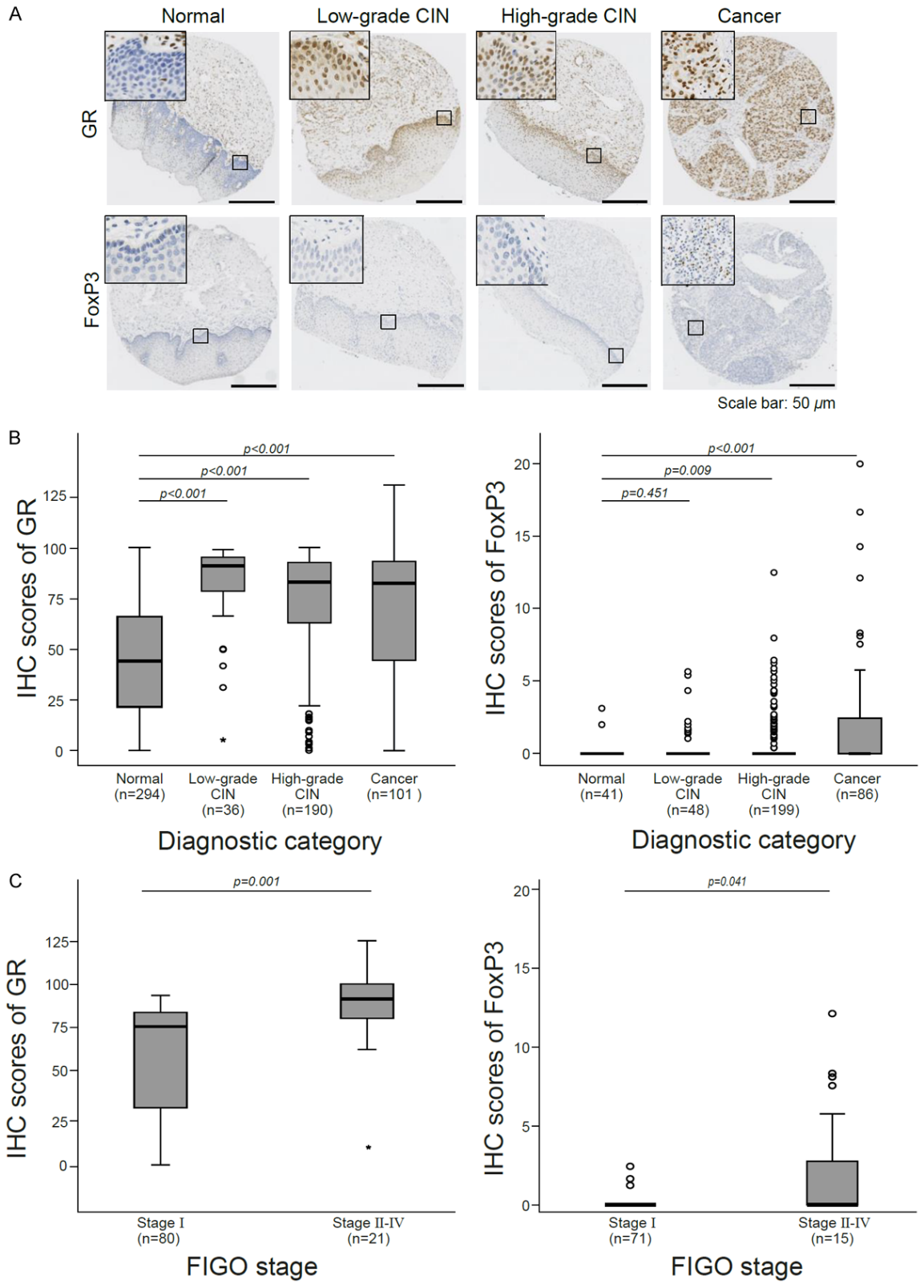

Figure 1. Determining GR or FoxP3 expression in cervical cancer specimen. A tissue microarray (TMA) containing 188 cervical cancer, 218 high-grade CIN, 102 low-grade CIN specimens, and 300 non-adjacent normal cervical epithelia were stained to confirm the expression of GR or FoxP3. However, due to loss of spot while sectioning, 101 cervical cancer, 190 high-grade CIN, 36 low-grade CIN specimens, and 294 nonadjacent normal cervical epithelia

were able to be interpreted for GR and 86 cervical cancer, 199 high-grade CIN, 48 low-grade CIN specimens, and 41 nonadjacent normal cervical epithelia were able to be interpreted for FoxP3. A. Representative immunohistochemical staining images of GR or FoxP3 (Scale bar 50 μm). B, C. Boxplots of IHC scores. The IHC staining score of GR or FoxP3 was significantly increased in cervical cancer specimens. In addition, their expression levels were significantly overexpressed in advanced FIGO stage.

Table 1. Association of GR and FoxP3 expression with clinicopathological characteristics in human cervical neoplasia

	GR			FoxP3		
	No.	Mean score (95% CI)	*P value*	No.	Mean score (95% CI)	*P value*
All study subjects						
Diagnostic category						
Normal	294	43.94 [40.72-47.16]	*< 0.001*	41	0.11 [0.03-0.19]	*< 0.001*
Low-grade CIN	36	81.34 [74.12-88.56]		48	0.6 [0.2-0.99]	
High-grade CIN	190	73.4 [69.67-77.13]		199	0.71 [0.48-0.95]	
Cancer	101	70.78 [64.01-77.55]		86	2.27 [1.18-3.36]	
FIGO stage			*< 0.001*			*0.041*
I	80	63.83 [56.41-71.25]		71	0.35 [-0.07-0.78]	
II-IV	21	93.1 [82.35-103.85]		15	2.64 [1.35-3.93]	
Tumor grade			*0.415*			*0.491*
Well/Moderate	53	66.95 [57.23-76.68]		43	2.71 [0.8-4.62]	
Poor	31	71.95 [60.28-83.62]		27	1.14 [0.4-1.89]	
Cell type			*0.278*			*0.543*
SCC	84	71.05 [63.87-78.23]		72	2.47 [1.21-3.73]	
Others	17	62.27 [44.32-80.21]		13	0.95 [-0.03-1.92]	
Tumor size			*0.051*			*0.226*
≤ 4 cm	80	66.92 [59.28-74.57]		72	2.5 [1.23-3.77]	
> 4 cm	21	79.66 [67.02-92.29]		14	0.98 [-0.15-2.12]	
LN metastasis			*0.64*			*0.525*
No	81	69 [61.72-76.29]		72	2.53 [1.25-3.8]	
Yes	18	71.63 [52.8-90.45]		11	0.96 [-0.01-1.93]	
Chemoradiation response			*0.041*			*0.731*
Good	33	71.04 [59.28-82.8]		26	1.8 [0.12-3.48]	
Bad	8	103.93 [58.97-149.18]		4	1.14 [-2.48-4.75]	
SCC antigen			*0.38*			*0.175*
Negative	54	65.47 [56.06-74.88]		47	2.42 [0.73-4.11]	
Positive	18	70.87 [51.07-90.68]		11	2.08 [-1.96-6.11]	
HPV test in CIN			*0.704*			*0.462*
Negative	23	74.86 [63.24-86.48]		25	0.71 [-0.14-1.56]	
Positive	203	71.44 [67.37-75.52]		222	1.03 [0.6-1.45]	

SCC, squamous cell carcinoma; FIGO, International Federation of Gynecology and Obstetrics; LN metastasis, Lymph node metastasis. Protein expression was determined through analysis of an immunohistochemically stained tissue array, as described in the materials and methods section.

cancer. GR overexpression (GR+) was related to poor DFS, and OS compared to low expression of GR (GR-) significantly (both $P < 0.001$; **Figure 2A**, **2B**). Like GR, FoxP3 overexpression (FoxP3+) was also observed in patient with poor DFS, and OS compared to low expression of FoxP3 (FoxP3-; $P = 0.013$, $P = 0.019$, respectively; **Figure 2C**, **2D**).

After investigating the prognostic value of a GR or FoxP3 individually, we compared the DFS and OS of patients with both GR and FoxP3

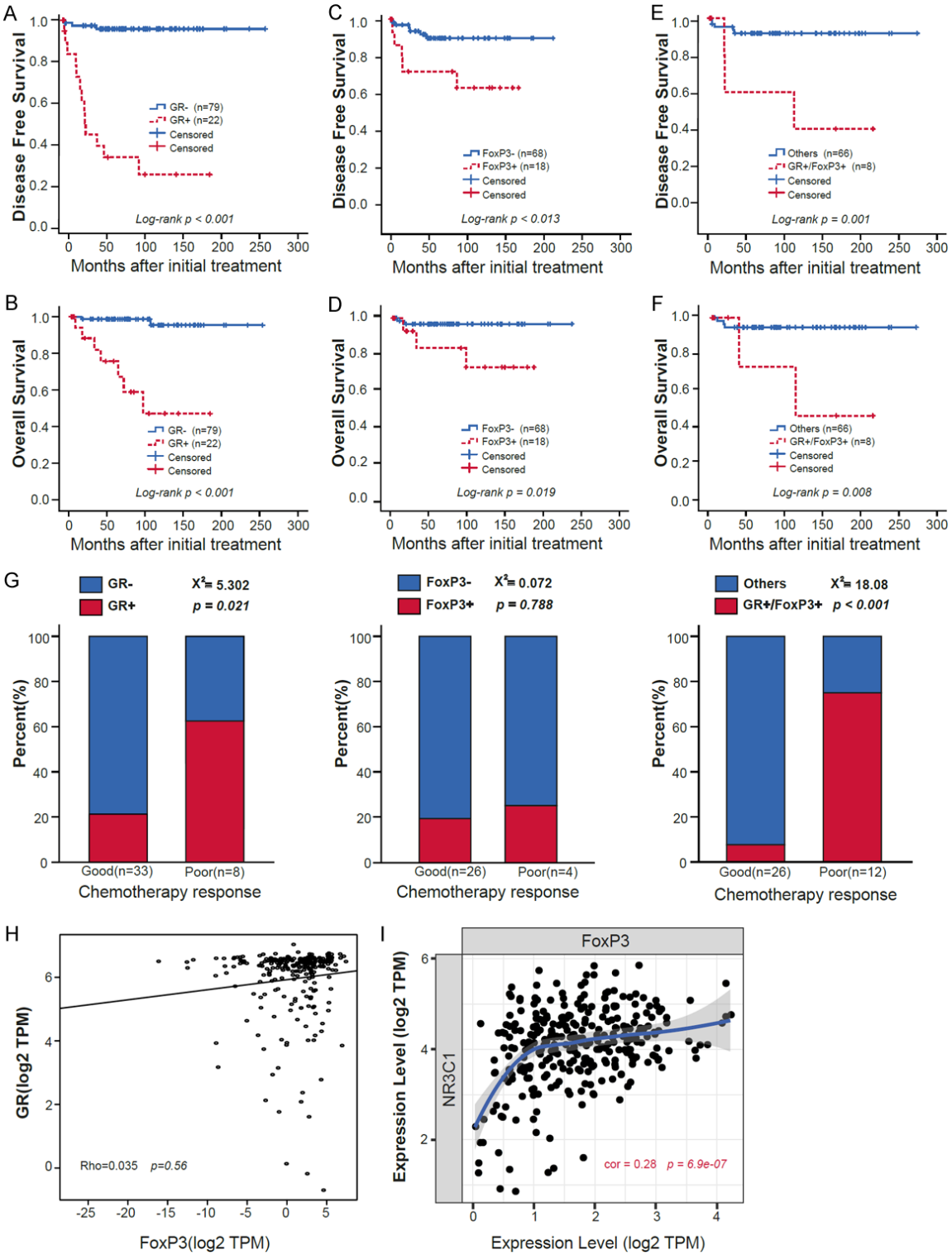

Figure 2. Kaplan-Meier survival curve of GR or FoxP3 expression in cervical cancer specimen. A-F. Kaplan-Meier plot indicating the disease-free survival or overall survival categorized by GR or FoxP3 expression in patients with cervical cancer. G. The bar graph indicating the response to chemoradiation therapy categorized by GR or FoxP3 or combination of GR and FoxP3 expression in patients with cervical cancer. H. The correlation between GR and FoxP3 expression in patients with cervical cancer in our study samples. I. The correlation of GR with FoxP3 expression estimated by TIMER 2.0 in patients with cervical cancer.

overexpression (GR+/FoxP3+), as previous studies reported that GR was upregulated during Treg cell differentiation, and that glucocorticoid-responsive *GILz* promotes Treg cell differentiation. Our study showed significantly poorer DFS and OS in patients with GR+/FoxP3+ expression than in other patients (P = 0.001 and P = 0.008, respectively; **Figure 2E**, **2F**). Furthermore, after performing the Cox proportional hazard model for DFS and OS, multivariate analysis revealed that, even though GR expression served as an independent risk factor for DFS and OS. Moreover, interestingly, the combination of GR and FoxP3 (GR+/FoxP3+), was the most strongly related risk factor for both DFS and OS in cervical cancer (HR = 29.16, 95% CI = 1.65-515.69, P = 0.021; and HR = 26.35, 95% CI = 1.11-626.5, P = 0.043; **Table 2**). In totality, these results suggest that in patients with cervical cancer, the combined overexpression of GR and FoxP3 is a significant prognostic marker.

As GR+/FoxP3+ was found to be a more valuable predictive biomarker for OS and DFS in cervical cancer, we further validated the clinicopathological characteristics. Notably, the combination of GR+ and FoxP3+ (GR+/FoxP3+) showed a higher predictive value for poor chemotherapy response than the single protein expression (P < 0.001; **Figure 2G**). To further verify the association between GR and FoxP3 in cervical cancer specimens, we performed Spearman's rank correlation analysis which did not build a significant correlation in our cervical cancer specimens (Spearman's rho = 0.035, P = 0.56). However, we noted the significant positive correlation between GR and FoxP3 in cervical cancer from TIMER2.0, a comprehensive resource platform of purity (**Figure 2I**). The discordance may be due to protein stability [23]. Hence, GR+/FoxP3+ may predict the response to CCRT in cervical cancer patients who are at a high risk of relapse, similar to their use as a predictive biomarker for poor prognosis.

Knockdown of GR expression enhances chemosensitivity to various anti-cancer agents including cisplatin in cervical cancer cells

Since GR is known to mediate resistance to both targeted therapies and conventional chemotherapies in a variety of epithelial cancers and in our study sample, we examined whether knockdown of endogenous GR expression could enhance the chemosensitivity of cervical cancer cells [24, 25]. The expression of GR was markedly reduced by siGR in Caski and SiHa cells (**Figure 3A**). To determine whether the knockdown of GR expression altered apoptosis induced by chemotherapeutic drugs, e.g., cisplatin, carboplatin, and 5-fluorouracil (5-FU), we measured the apoptotic cell population with FACS-based Annexin-V/PI double staining. siGR-transfected cells were highly sensitive to cisplatin-induced apoptosis (**Figure 3B**, Supplementary Figure 1A) and increased cleavage of poly (ADP-ribose) polymerase (PARP) (**Figure 3C**, Supplementary Figure 1B). We then assessed the impact of ligand-dependent GR activation on anticancer drugs resistance, and ligand stimulation with dexamethasone (DEX) significantly prevented the anticancer drugs-induced apoptosis in Caski and SiHa cells (Supplementary Figure 2A, 2B). These results suggest that GR contributes to the chemoresistance of cervical cancer cells against anticancer drugs-induced apoptosis.

Suppression of p38 MAP kinase is critical for the GR-mediated resistance to cisplatin

Next, we further questioned how GR mediates resistance to cisplatin. To address this issue, we examined p38 MAP kinase activity in cervical cancer cells after treatment with cisplatin, as previous studies have reported that the stress-activated kinase p38 MAP kinase were related to cisplatin cytotoxicity in other cancer cell lines [26]. As shown in **Figure 4A**, the phosphorylation level of p38 was significantly increased in siGR-transfected cells compared with control cells (siControl) in response to cisplatin. To further investigate whether GR modulates cisplatin resistance through p38 MAP kinase, we tested whether inhibition of p38 activity affects cisplatin-induced apoptosis in siGR-transfected cells. The results showed that the blocking p38 activity by SB203580 significantly diminished cisplatin-induced apoptosis (**Figure 4B**) and decreased cleaved PARP (**Figure 4C**) in siGR-transfected cells. These results indicate that suppression of p38 activity is crucial for GR-mediated cisplatin resistance in cervical cancer cells.

Table 2. Univariate and multivariate analyses of disease free survival or overall survival in cervical cancer patients

Variables	Disease free survival				Overall survival			
	Univariate analysis		Multivariate analysis		Univariate analysis		Multivariate analysis	
	Hazard ratio [95% CI]	*P* value	Hazard ratio [95% CI]	*P* value	Hazard ratio [95% CI]	*P* value	Hazard ratio [95% CI]	*P* value
Age (> 50)	1.49 [0.83-2.67]	0.181	NA		0.78 [0.33-1.82]	0.567	NA	
FIGO stage (> IIA)	6.72 [3.59-12.58]	< 0.001	2.59 [0.35-19.28]	0.352	4.15 [1.84-9.38]	0.001	1.14 [0.09-14.79]	0.921
Grade (poor)	1.73 [0.96-3.12]	0.070	NA		2.03 [0.90-4.61]	0.090	NA	
Cell type (non-SCC)	1.03 [0.48-2.21]	0.939	NA		2.48 [1.06-5.8]	0.036	1.11 [0.10-12.31]	0.930
Tumor size (> 4 cm)	2.31 [1.27-4.18]	0.006	0.91 [0.25-3.35]	0.889	1.96 [0.85-4.51]	0.114	NA	
LN metastasis	3.97 [2.00-7.88]	< 0.001	2.40 [1.01-5.70]	0.046	2.69 [1.06-6.86]	0.038	1.92 [0.34-10.88]	0.462
SCC Ag^+	2.38 [1.26-4.52]	0.008	2.77 [0.80-9.67]	0.109	2.78 [1.18-6.55]	0.020	4.28 [0.62-29.66]	0.141
GR^{+a}	25.71 [8.69-76.08]	< 0.001	11.73 [2.18-63.22]	0.004	12.31 [3.05-49.75]	< 0.001	13.54 [1.25-146.88]	0.032
$FoxP3^{+b}$	4.61 [1.45-14.66]	0.010	1191910318.54 [0-Inf]	0.999	6.5 [1.07-39.26]	0.042	4774920538.83 [0-Inf]	0.999
$GR^+/FoxP3^{+-}$	5.91 [1.18-29.61]	0.031	29.16 [1.65-515.69]	0.021	3.93 [0.44-35.21]	0.221	26.35 [1.11-626.5]	0.043

[a]cut-off value of GR^+ is over 101.01 of IHC score; [b]cut-off of $FoxP3^+$ is over 4.08 of IHC score; CI, confidence interval; FIGO, International Federation of Gynecology and Obstetrics; LN, lymph node; NA, not applicable.

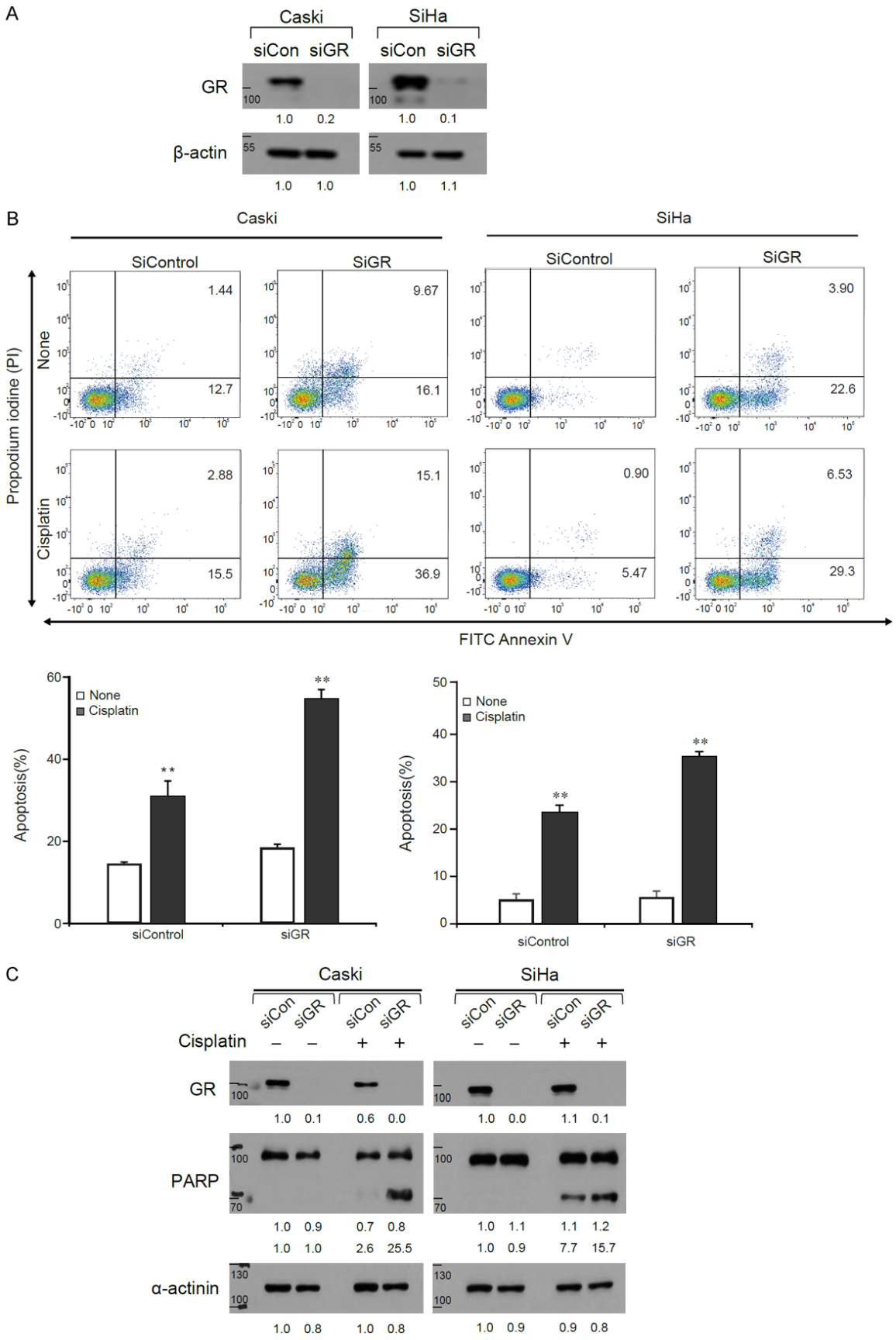
A
Caski
SiHa
siCon siGR
siCon siGR
GR
100
1.0 0.2
1.0 0.1
β-actin
55
1.0 1.0
1.0 1.1
B
Caski
SiHa
SiControl
SiGR
SiControl
SiGR
Propodium iodine (PI)
None
Cisplatin
1.44
9.67
3.90
12.7
16.1
22.6
2.88
15.1
0.90
6.53
15.5
36.9
5.47
29.3
FITC Annexin V
Apoptosis(%)
None
Cisplatin
siControl
siGR
C
Caski
SiHa
siCon siGR siCon siGR
siCon siGR siCon siGR
Cisplatin – – + +
– – + +
GR
100
1.0 0.1 0.6 0.0
1.0 0.0 1.1 0.1
PARP
100
70
1.0 0.9 0.7 0.8
1.0 1.0 2.6 25.5
1.0 1.1 1.1 1.2
1.0 0.9 7.7 15.7
α-actinin
130
100
1.0 0.8 1.0 0.8
1.0 0.9 0.9 0.8

Figure 3. GR was knocked down in Caski and SiHa cells for 72 hr. A. Protein expression of GR and β-actin was analyzed by western blotting. B. Caski and SiHa cells were transfected with siRNA against GR for 48 hr followed by treatment with 20 μM cisplatin. Cells were harvested and apoptosis was analyzed using flow cytometry after staining with annexin V-FITC/propidium iodide. Upper panel: representative scatter plots of propidium iodide (y-axis) versus annexin V (x-axis). Lower panel: Quantitative analysis of apoptotic cells. Protein expression of GR, PARP, and α-actinin was analyzed by western blotting (numbers below each blot are densitometric values). C. Protein expression of PARP and β-actin was analyzed by western blotting (numbers below each blot are densitometric values). The number of asterisks (*) indicates the level of significance: **P < 0.05, ***P < 0.005. Error bars represent mean ± standard error of triplicate experiments.

Knockdown of GR expression or GR activation by its ligand alters the migration and invasion properties of cervical cancer cells

As GR promotes invasion of cancer cells [27-29] and enhances cisplatin resistance, we examined whether knockdown of GR or GR activation by its agonist affects the migration and invasive properties of cervical cancer cells. In this regard, we revealed significant diminution of migration (**Figure 5A**) and invasion (**Figure 5B**) in siGR-transfected cells compared to control cells by the Boyden chamber assay. Treatment with DEX greatly increased migration and invasion compared with untreated cells in Caski cells, but not SiHa cells (Supplementary Figure 3A, 3B). The difference between the results for Caski and SiHa cells may be due to the cell type. Next, we examined the effect of GR knockdown on the expression patterns of epithelial-mesenchymal transition (EMT) markers. siGR-transfected cells showed decreased expression of Slug and increased expression of E-cadherin (**Figure 5C**). Taken together, our results suggest that GR facilitates cervical cancer cell migration and invasion, and the EMT process of cervical cancer cells.

Knockdown of FoxP3 expression inhibits proliferation of cervical cancer cells

Our results proved that GR and FoxP3 were inseparable in their prognostic value, so we tested whether knockdown of GR expression affects FoxP3 expression in cervical cancer cells. As shown in **Figure 6A**, FoxP3 was downregulated in siGR-transfected cells compared to that in control cells (siControl).

We then investigated the effect of FoxP3 knockdown on several tumorigenic features of cervical cancer cells. Caski and SiHa cells were transfected with a specific siRNA (siFoxP3), and the silencing effect was validated by qPCR (**Figure 6B**). The cell proliferation assay showed that FoxP3 knockdown suppressed cell growth (**Figure 6C**). A colony formation assay was used to confirm the effect of FoxP3 on cervical cancer cell proliferation. As shown in **Figure 6D**, the number of colonies formed by siFOXP3-transfected cells was lower than that by the control cells. Based on these results, we confirmed the oncogenic property of FoxP3 in cervical cancer cell lines.

Discussion

GR has been in the spotlight of cancer research for decades, and compelling evidence supports the oncogenic role of GR in various solid malignancies. However, its role in cervical cancer is still not entirely understood. In the present study, we identified the clinical relevance of GR in cervical cancer, as GR is prominently overexpressed in cervical cancer, related to poor prognosis and poor response to CCRT. Furthermore, we investigated whether GR induced cisplatin resistance by inhibiting p38 MAP kinase activity and examined the association between GR and FoxP3 in cervical cancer cell lines, which have not been previously explored in cervical cancer.

Indeed, the oncogenic role of GR in various solid cancers has been a topic of interest lately. In hepatocellular carcinoma (HCC), cancerous tissues were shown to have GR overexpression in comparison to regions of normal epithelia, and was associated with unfavorable prognosis [30]. Further studies in EOC and endometrial cancer have also reported that overexpression of GR was associated with an unfavorable prognosis [31, 32]. However, there are limited data on the overexpression of GR in cervical cancer and its association with prognosis. As such, in this study we explored the expression of GR in cervical cancer. Furthermore, we utilized samples from a large patient cohort (cervical cancer, precursor, and normal tissue) to investigate the clinical value of GR and found that GR was significantly upregulated in cervical cancer tissues compared to their corresponding nor-

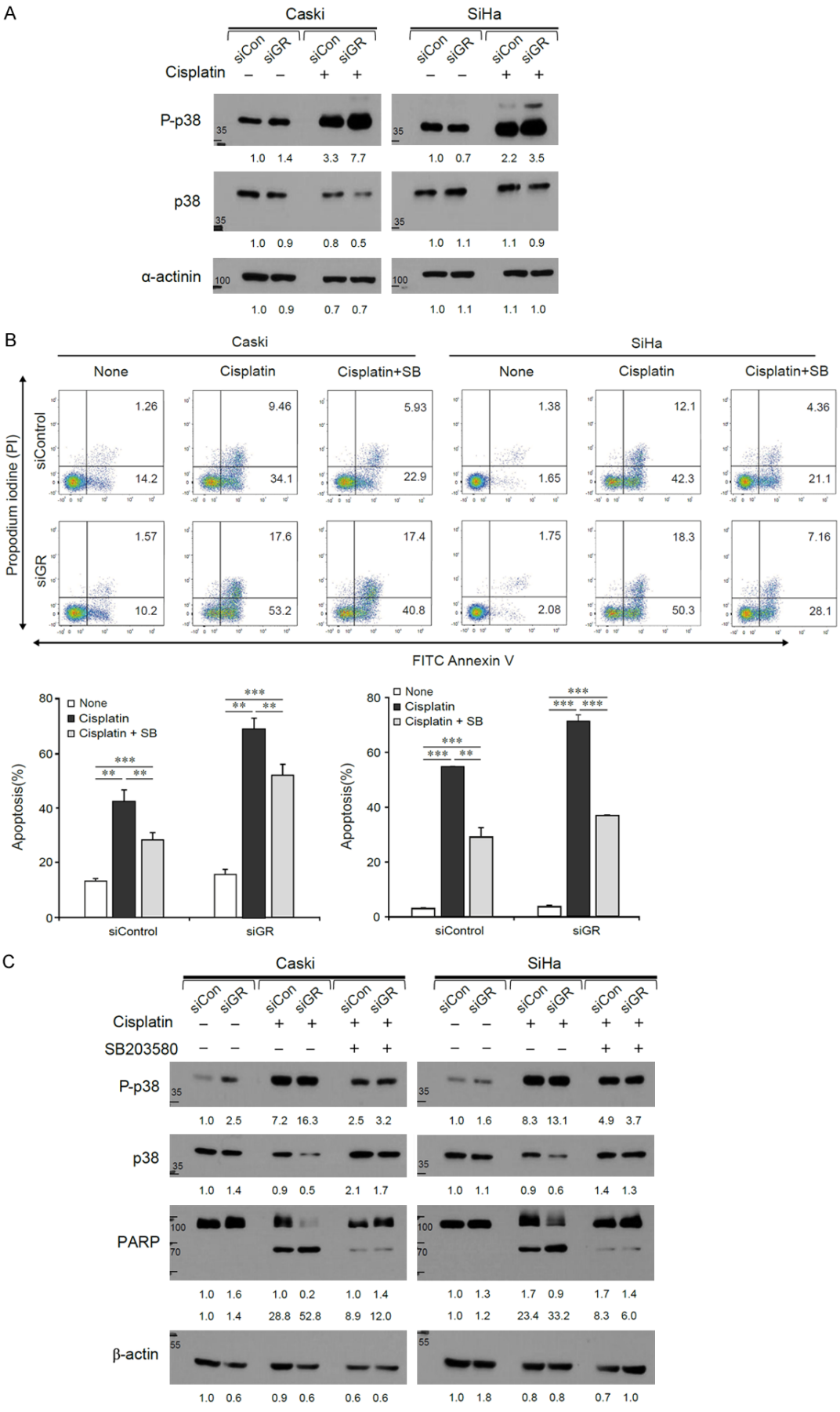
A
Caski
SiHa
siCon
siGR
Cisplatin
P-p38
p38
α-actinin
B
Caski
SiHa
None
Cisplatin
Cisplatin+SB
siControl
siGR
Propodium iodine (PI)
FITC Annexin V
Apoptosis(%)
C
SB203580
PARP
β-actin

Figure 4. Suppression of p38 MAP kinase is critical for the GR-mediated resistance to cisplatin. Caski and SiHa cells were transfected with siRNA against GR for 48 hr. Cells were pretreated with 10 μM SB203580 for 1 hr, and then incubated with 20 μM cisplatin for 24 hr. A. Protein expression of P-p38, p38, and β-actin was analyzed by western blotting. B. The apoptosis was analyzed with flow cytometry after staining with annexin V-FITC/propidium iodide. Upper panel: representative scatter plots of propidium iodide (y-axis) versus annexin V (x-axis). Lower panel: Quantitative analysis of apoptotic cells. C. Protein expression of P-p38, p38, PARP, and β-actin was analyzed by western blotting. The number of asterisks (*) indicates the level of significance: **P < 0.05, ***P < 0.005. Error bars represent mean ± standard error of triplicate experiments.

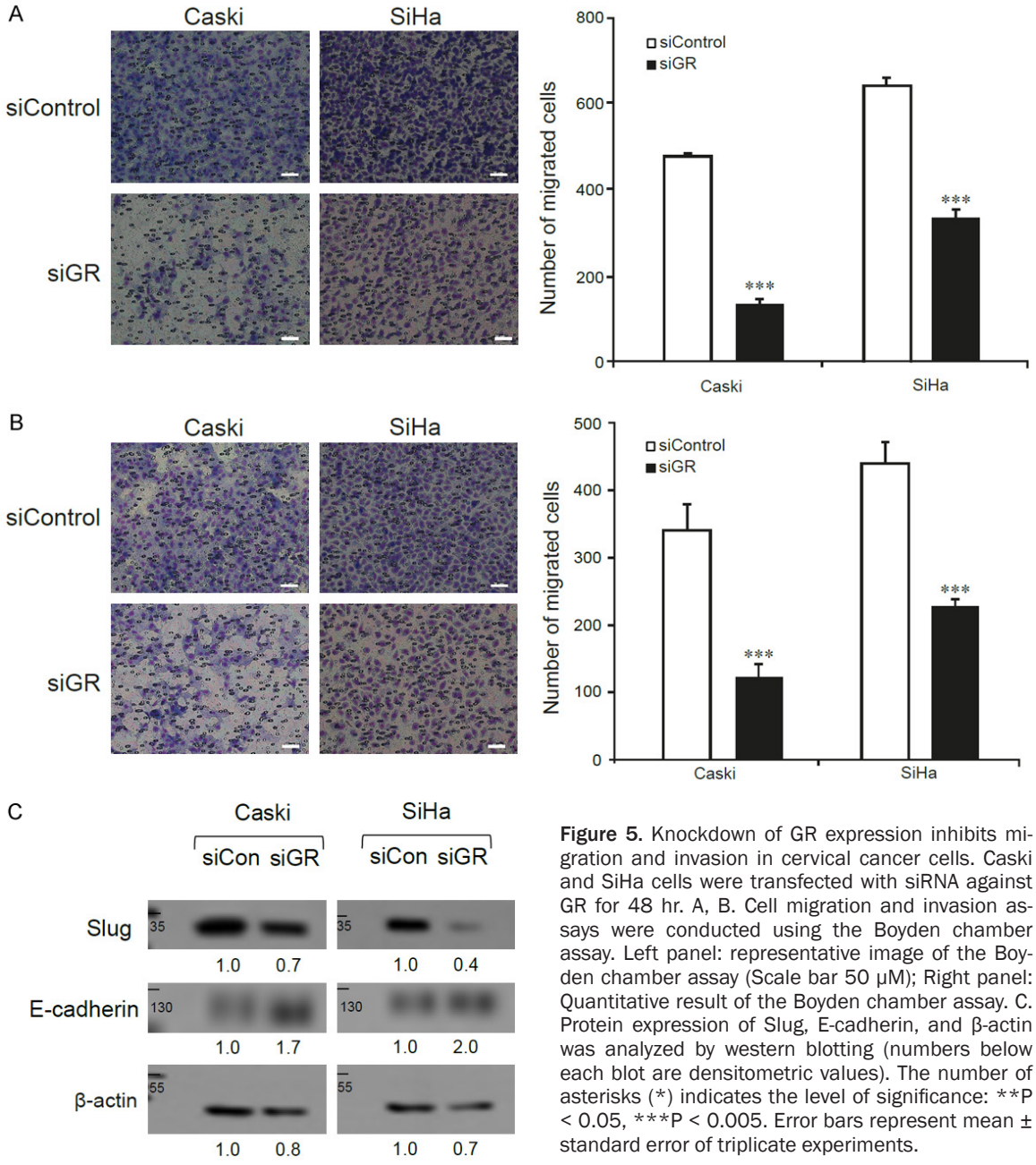

Figure 5. Knockdown of GR expression inhibits migration and invasion in cervical cancer cells. Caski and SiHa cells were transfected with siRNA against GR for 48 hr. A, B. Cell migration and invasion assays were conducted using the Boyden chamber assay. Left panel: representative image of the Boyden chamber assay (Scale bar 50 μM); Right panel: Quantitative result of the Boyden chamber assay. C. Protein expression of Slug, E-cadherin, and β-actin was analyzed by western blotting (numbers below each blot are densitometric values). The number of asterisks (*) indicates the level of significance: **P < 0.05, ***P < 0.005. Error bars represent mean ± standard error of triplicate experiments.

mal tissues. Notably, we found that overexpression of GR was observed in both cervical cancer precursors (low-grade and high-grade CIN) and invasive cancer, which may suggest that GR has some utility in screening even in which precursor lesions that are highly likely to develop into invasive cervical cancer. However, while our data is consistent with some previously

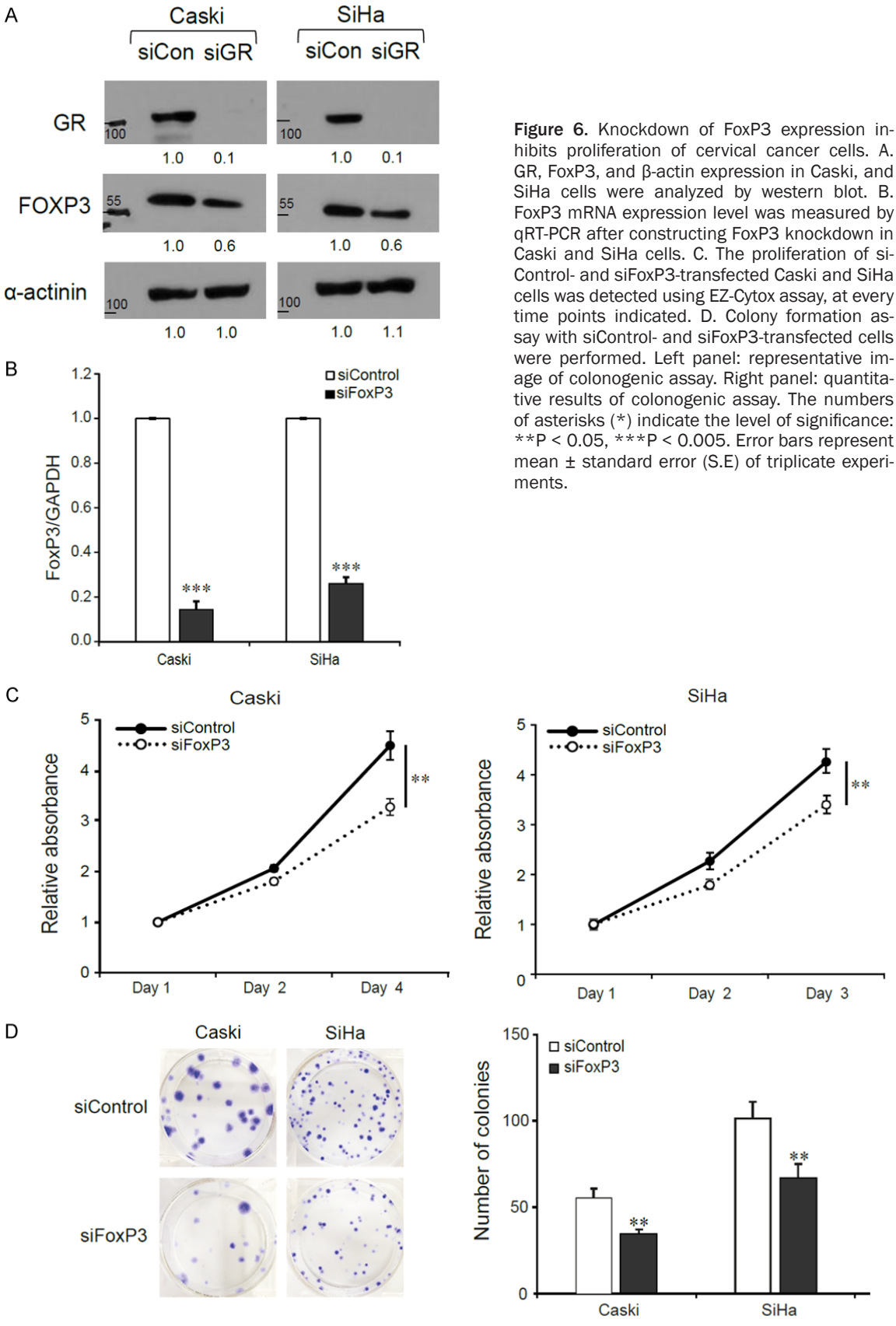

Figure 6. Knockdown of FoxP3 expression inhibits proliferation of cervical cancer cells. A. GR, FoxP3, and β-actin expression in Caski, and SiHa cells were analyzed by western blot. B. FoxP3 mRNA expression level was measured by qRT-PCR after constructing FoxP3 knockdown in Caski and SiHa cells. C. The proliferation of si-Control- and siFoxP3-transfected Caski and SiHa cells was detected using EZ-Cytox assay, at every time points indicated. D. Colony formation assay with siControl- and siFoxP3-transfected cells were performed. Left panel: representative image of colonogenic assay. Right panel: quantitative results of colonogenic assay. The numbers of asterisks (*) indicate the level of significance: **P < 0.05, ***P < 0.005. Error bars represent mean ± standard error (S.E) of triplicate experiments.

published data about GR expression in cervical cancer tissues, the studies are not unanimous [33]. For instance, Kost *et al*. [34] reported that overexpression of GR in cervical cancer is correlated with better DFS and OS. Although our study and Kost *et al*. performed IHC to evaluate GR, and measured GR staining intensity in the nucleus, there are several potential factors contributing to this discordance, including the scoring and threshold for the definition of overexpression, IHC methodology, and selection of patients. Of note, our study reinforced the methodological strength by applying automated digital image analysis rather than manual interpretation as the automated digital image analysis provides more reproducible, objective result with less intra-inter-pathologist inconsistency [35]. Also, as we used the nonadjacent normal cervical epithelial tisseus for control, they used normal placenta tissues for the control which may also strenthens our study.

Glucocorticoids are commonly utilized to treat side effects of chemotherapy and symptoms of cancer at advanced stages. Seemingly paradoxically, GR expression has been previously shown to prevent therapy response and apoptosis in variety of epithelial cancers, such as cancers of the breast, ovary (11), testis, prostate, kidney, bladder (37), brain (38, 39), colon, and liver (40). In light of this, our study found that GR overexpression is associated with a poor response to chemoradiation therapy in cervical cancer clinical specimens and that GR knockdown enhanced apoptosis by anti-cancer agents such as cisplatin, carboplatin, and 5-FU, which was demonstrated by significant increases in apoptotic marker expression. The overexpression of GR has been previously observed in cancer cells with poor response to chemotherapy, and the underlying mechanism responsible for linking overexpression to acquisition of resistance is largely unknown. According to a study on breast cancer cell lines, the cisplatin-induced pro-apoptotic effect in several tumors is accompanied by p38 activation via phosphorylation [36]. In addition, Huang *et al*. [31] used FACS and Hoechst staining in lung cancer cells to demonstrate the phosphorylation and dephosphorylation of p38 by cisplatin and dexamethasone, respectively, validating that via p38 dephosphorylation and inactivation by MPK-1, the anti-apoptotic process controls cytotoxicity resistance induced by dexamethasone. To prove this principle in cervical cancer, we found that GR knockdown profoundly upregulated phosphorylated-p38 MAPK by administering cisplatin, suggesting that GR expression promotes resistance to cisplatin in cervical cancer cell lines. We further confirmed this result by using the p38 MAPK inhibitor SB-203580, which markedly blocked the induction of phophos-p38, resulting in increased sensitivity of cervical cancer cells to cisplatin in siGR-transfected cervical cancer cell lines. We used molecular and cellular technology to demonstrate the interaction between GR and p38 MAPK in association with cisplatin resistance, but the signal transduction pathway for apoptosis in response to cytotoxic stress, particularly in the reported link between MAPK activation and downstream effects mediated by GR, remains inconclusive. Many studies have shown MAPK members ERK, p38, and JNK to have differing activation profiles in response to cytotoxic stress (42). As such, to comprehend the mechanism responsible for chemoresistance induced by glucocorticoids, further studies must be done on the link between several signaling molecules.

EMT is known as an essential process for cancer migration and invasion and acquisition of chemoresistance [37, 38]. Our additional experiments showed that siRNA-mediated GR knockdown drastically decreased cell migration, invasion, and rendered expression of EMT markers, slug and E-cadherin, supporting the notion that GR promotes EMT in cervical cancer cells. A series of functional studies in breast cancer showed that, as evidenced by cell migration, EMT, and enhanced expression of vimentin and AP-1, RAS/JNK activity did not trigger apoptosis [39]. In addition, Liu *et al*. [40] reported the effect of GR on metastasis by demonstrating that dexamethasone-mediated effects were partly undone by the inhibition of either JNK, TGFβ receptor-1, or GR signaling, implying that there exists an intricate signaling network. Our study advanced the understanding of the role of GR in partially regulating cervical cancer metastasis through EMT. Further study would be interesting to clarify the molecular basis of the regulation of the GR signaling pathway and its downstream target genes during metastasis.

In addition to the role of GR in chemotherapy resistance, we further confirmed that GR mediates the expression of FoxP3 in cervical cancer

cell lines by western blotting. Notably, we demonstrated that the combination of GR and FoxP3 overexpression is an important prognostic factor in patients with cervical cancer with the highest hazard ratio and predicts response to CCRT. Previous studies on the effect of GR on T cell differentiation demonstrated that GR overexpression reduced the number of T helper cells by approximately half, but increased the proportion of Treg cells [41]. Moreover, Ugor *et al.* [42]. reported that colocalization of GR and FoxP3 was increased upon dexamethasone treatment, suggesting that regions of chromatin may recruit transcription factors for GR and FoxP3, while gene transcription may be modulated either in tandem or independently. Besides in mammalian cells, the FoxP3 gene was found to have a region that binds GR (49). However, how GR modulated expression of FoxP3 in various cancer including cervical cancer need further research to substantiate the relationship between FoxP3 and GR signaling. We showed that GR modulates the phosphorylation of p38. In light of these findings and previous research by Lu *et al*. [43] which reported that p38 MAPK signaling contributed to the conversion of effector T (Teff) cells to Treg, we propose that the p38 MAPK signaling pathway is the important regulator between GR and FoxP3 in cervical cancer cells.

Conclusion

In conclusion, our study established that overexpression of GR was associated with both poor prognosis and platinum-based chemotherapy resistance in cervical cancer patients. Of note, the combination of overexpression of GR and FoxP3 showed the possibility of being an even stronger predictive biomarker for prognosis and poor response to CCRT in cervical cancer patients. Functionally, we have demonstrated that GR induces platinum-based chemotherapy resistance via the p38 MAPK signaling pathway in GR-knockdown cervical cancer cell lines and suggested the pivotal role of GR and FoxP3 in cervical cancer patients in terms of providing prognostic predictive value as well as being a biomarker for precision medicine in determining a therapeutic strategy.

Acknowledgements

This work was supported by the National Research Foundation of Korea (NRF) grant funded by the Korea government (MIST) (NRF-2020R1A2C2004782). This research was supported by the Bio & Medical Technology Development Program of the National Research Foundation (NRF) funded by the Korean government (MSIT) (NRF-2017M3A9B8 069610). This study was also supported by a faculty research grant of Yonsei University College of Medicine (No. 6-2020-0226).

Informed consent has been obtained from the participants prior to surgery to use their tissue as materials in research.

Disclosure of conflict of interest

None.

Address correspondence to: Dr. Hanbyoul Cho, Department of Obstetrics and Gynecology, Gangnam Severance Hospital, Yonsei University College of Medicine, 211 Eonju-Ro, Gangnam-Gu, Seoul 06273, Republic of Korea. Tel: +82-2-2019-3430; Fax: +82-2-3462-8209; E-mail: hanbyoul@yuhs.ac

References

[1] Sung H, Ferlay J, Siegel RL, Laversanne M, Soerjomataram I, Jemal A and Bray F. Global cancer statistics 2020: GLOBOCAN estimates of incidence and mortality worldwide for 36 cancers in 185 countries. CA Cancer J Clin 2021; 71: 209-249.

[2] Burd EM. Human papillomavirus and cervical cancer. Clin Microbiol Rev 2003; 16: 1-17.

[3] Kalliala I, Athanasiou A, Veroniki A, Salanti G, Efthimiou O, Raftis N, Bowden S, Paraskevaidi M, Aro K and Arbyn M. Incidence and mortality from cervical cancer and other malignancies after treatment of cervical intraepithelial neoplasia: a systematic review and meta-analysis of the literature. Ann Oncol 2020; 31: 213-227.

[4] Kassel O and Herrlich P. Crosstalk between the glucocorticoid receptor and other transcription factors: molecular aspects. Mol Cell Endocrinol 2007; 275: 13-29.

[5] Weikum ER, Knuesel MT, Ortlund EA and Yamamoto KR. Glucocorticoid receptor control of transcription: precision and plasticity via allostery. Nat Rev Mol Cell Bio 2017; 18: 159-174.

[6] Pan D, Kocherginsky M and Conzen SD. Activation of the glucocorticoid receptor is associated with poor prognosis in estrogen receptor-negative breast cancer. Cancer Res 2011; 71: 6360-6370.

[7] Skor MN, Wonder EL, Kocherginsky M, Goyal A, Hall BA, Cai Y and Conzen SD. Glucocorticoid

receptor antagonism as a novel therapy for triple-negative breast cancer. Clin Cancer Res 2013; 19: 6163-6172.
[8] Zhang C, Kolb A, Büchler P, Cato AC, Mattern J, Rittgen W, Edler L, Debatin KM, Büchler MW and Friess H. Corticosteroid co-treatment induces resistance to chemotherapy in surgical resections, xenografts and established cell lines of pancreatic cancer. BMC Cancer 2006; 6: 1-14.
[9] Stringer-Reasor EM, Baker GM, Skor MN, Kocherginsky M, Lengyel E, Fleming GF and Conzen SD. Glucocorticoid receptor activation inhibits chemotherapy-induced cell death in high-grade serous ovarian carcinoma. Gynecol Oncol 2015; 138: 656-662.
[10] Zhang C, Marmé A, Wenger T, Gutwein P, Edler L, Rittgen W, Debatin KM, Altevogt P, Mattern J and Herr I. Glucocorticoid-mediated inhibition of chemotherapy in ovarian carcinomas. Int J Oncol 2006; 28: 551-558.
[11] Sui M, Chen F, Chen Z and Fan W. Glucocorticoids interfere with therapeutic efficacy of paclitaxel against human breast and ovarian xenograft tumors. Int J Cancer 2006; 119: 712-717.
[12] Pang D, Kocherginsky M, Krausz T, Kim SY and Conzen SD. Dexamethasone decreases xenograft response to Paclitaxel through inhibition of tumor cell apoptosis. Cancer Biol Ther 2006; 5: 933-940.
[13] Weigel D, Jürgens G, Küttner F, Seifert E and Jäckle H. The homeotic gene fork head encodes a nuclear protein and is expressed in the terminal regions of the Drosophila embryo. Cell 1989; 57: 645-658.
[14] Leffers N, Gooden MJ, de Jong RA, Hoogeboom BN, ten Hoor KA, Hollema H, Boezen HM, van der Zee AG, Daemen T and Nijman HW. Prognostic significance of tumor-infiltrating T-lymphocytes in primary and metastatic lesions of advanced stage ovarian cancer. Cancer Immunol Immunother 2009; 58: 449-459.
[15] Wicherek L, Jozwicki W, Windorbska W, Roszkowski K, Lukaszewska E, Wisniewski M, Brozyna AA, Basta P, Skret-Magierlo J and Koper K. Analysis of Treg cell population alterations in the peripheral blood of patients treated surgically for ovarian cancer-a preliminary report. Am J Reprod Immunol 2011; 66: 444-450.
[16] Song JJ, Zhao SJ, Fang J, Ma D, Liu XQ, Chen XB, Wang Y, Cheng B and Wang Z. Foxp3 overexpression in tumor cells predicts poor survival in oral squamous cell carcinoma. BMC Cancer 2016; 16: 530.
[17] Lee S, Cho EY, Park YH, Ahn JS and Im YH. Prognostic impact of FOXP3 expression in triple-negative breast cancer. Acta Oncol 2013; 52: 73-81.
[18] Zuo T, Liu R, Zhang H, Chang X, Liu Y, Wang L, Zheng P and Liu Y. FOXP3 is a novel transcriptional repressor for the breast cancer oncogene SKP2. J Clin Invest 2007; 117: 3765-3773.
[19] Zuo T, Wang L, Morrison C, Chang X, Zhang H, Li W, Liu Y, Wang Y, Liu X, Chan MW, Liu JQ, Love R, Liu CG, Godfrey V, Shen R, Huang TH, Yang T, Park BK, Wang CY, Zheng P and Liu Y. FOXP3 is an X-linked breast cancer suppressor gene and an important repressor of the HER-2/ErbB2 oncogene. Cell 2007; 129: 1275-1286.
[20] Luo Q, Zhang S, Wei H, Pang X and Zhang H. Roles of Foxp3 in the occurrence and development of cervical cancer. Int J Clin Exp Pathol 2015; 8: 8717-8730.
[21] Matsuo K, Machida H, Mandelbaum RS, Konishi I and Mikami M. Validation of the 2018 FIGO cervical cancer staging system. Gynecol Oncol 2019; 152: 87-93.
[22] Li T, Fu J, Zeng Z, Cohen D, Li J, Chen Q, Li B and Liu XS. TIMER2. 0 for analysis of tumor-infiltrating immune cells. Nucleic Acids Res 2020; 48: W509-W514.
[23] Duma D, Jewell CM and Cidlowski JA. Multiple glucocorticoid receptor isoforms and mechanisms of post-translational modification. J Steroid Biochem Mol Biol 2006; 102: 11-21.
[24] Pan C, Kang J, Hwang JS, Li J, Boese AC, Wang X, Yang L, Boggon TJ, Chen GZ, Saba NF, Shin DM, Magliocca KR, Jin L and Kang S. Cisplatin-mediated activation of glucocorticoid receptor induces platinum resistance via MAST1. Nat Commun 2021; 12: 4960.
[25] Zhang C, Wenger T, Mattern J, Ilea S, Frey C, Gutwein P, Altevogt P, Bodenmüller W, Gassler N, Schnabel PA, Dienemann H, Marmé A, Hohenfellner M, Haferkamp A, Pfitzenmaier J, Gröne HJ, Kolb A, Büchler P, Büchler M, Friess H, Rittgen W, Edler L, Debatin KM, Krammer PH, Rutz HP and Herr I. Clinical and mechanistic aspects of glucocorticoid-induced chemotherapy resistance in the majority of solid tumors. Cancer Biol Ther 2007; 6: 278-287.
[26] Hernandez Losa J, Parada Cobo C, Guinea Viniegra J, Sanchez-Arevalo Lobo VJ, Ramon y Cajal S and Sanchez-Prieto R. Role of the p38 MAPK pathway in cisplatin-based therapy. Oncogene 2003; 22: 3998-4006.
[27] Tian D, Tian M, Han G and Li JL. Increased glucocorticoid receptor activity and proliferation in metastatic colon cancer. Sci Rep 2019; 9: 11257.
[28] Obradović MMS, Hamelin B, Manevski N, Couto JP, Sethi A, Coissieux MM, Münst S, Okamoto R, Kohler H, Schmidt A and Bentires-Alj M. Glucocorticoids promote breast cancer metastasis. Nature 2019; 567: 540-544.

[29] Perez Kerkvliet C, Dwyer AR, Diep CH, Oakley RH, Liddle C, Cidlowski JA and Lange CA. Glucocorticoid receptors are required effectors of TGFβ1-induced p38 MAPK signaling to advanced cancer phenotypes in triple-negative breast cancer. Breast Cancer Res 2020; 22: 39.
[30] Ho WL, Wu CC, Yeh DC, Chen JT, Huang CC, Lin YL, Liu TJ and P'Eng FK. Roles of the glucocorticoid receptor in resectable hepatocellular carcinoma. Surgery 2002; 131: 19-25.
[31] Bakour N, Moriarty F, Moore G, Robson T and Annett SL. Prognostic significance of glucocorticoid receptor expression in cancer: a systematic review and meta-analysis. Cancers (Basel) 2021; 13: 1649.
[32] Tangen IL, Veneris JT, Halle MK, Werner HM, Trovik J, Akslen LA, Salvesen HB, Conzen SD, Fleming GF and Krakstad C. Expression of glucocorticoid receptor is associated with aggressive primary endometrial cancer and increases from primary to metastatic lesions. Gynecol Oncol 2017; 147: 672-677.
[33] Biewenga P, Buist MR, Moerland PD, Ver Loren van Themaat E, van Kampen AH, ten Kate FJ and Baas F. Gene expression in early stage cervical cancer. Gynecol Oncol 2008; 108: 520-526.
[34] Kost BP, Beyer S, Schröder L, Zhou J, Mayr D, Kuhn C, Schulze S, Hofmann S, Mahner S, Jeschke U and Heidegger H. Glucocorticoid receptor in cervical cancer: an immunhistochemical analysis. Arch Gynecol Obstet 2019; 299: 203-209.
[35] Grunkin M, Raundahl J and Foged NT. Practical considerations of image analysis and quantification of signal transduction IHC staining. Methods Mol Biol 2011; 717: 143-154.
[36] Pereira L, Igea A, Canovas B, Dolado I and Nebreda AR. Inhibition of p38 MAPK sensitizes tumour cells to cisplatin-induced apoptosis mediated by reactive oxygen species and JNK. EMBO Mol Med 2013; 5: 1759-1774.
[37] Taube JH, Herschkowitz JI, Komurov K, Zhou AY, Gupta S, Yang J, Hartwell K, Onder TT, Gupta PB, Evans KW, Hollier BG, Ram PT, Lander ES, Rosen JM, Weinberg RA and Mani SA. Core epithelial-to-mesenchymal transition interactome gene-expression signature is associated with claudin-low and metaplastic breast cancer subtypes. Proc Natl Acad Sci U S A 2010; 107: 15449-15454.
[38] Kalluri R and Weinberg RA. The basics of epithelial-mesenchymal transition. J Clin Invest 2009; 119: 1420-1428.
[39] Shi W, Wang D, Yuan X, Liu Y, Guo X, Li J and Song J. Glucocorticoid receptor-IRS-1 axis controls EMT and the metastasis of breast cancers. J Mol Cell Biol 2019; 11: 1042-1055.
[40] Liu L, Aleksandrowicz E, Schonsiegel F, Groner D, Bauer N, Nwaeburu CC, Zhao Z, Gladkich J, Hoppe-Tichy T, Yefenof E, Hackert T, Strobel O and Herr I. Dexamethasone mediates pancreatic cancer progression by glucocorticoid receptor, TGFbeta and JNK/AP-1. Cell Death Dis 2017; 8: e3064.
[41] Yakimchuk K, Chen L, Hasni MS, Okret S and Jondal M. The selective impact of transgenically expressed glucocorticoid receptor on T cells. Autoimmunity 2015; 48: 117-124.
[42] Ugor E, Prenek L, Pap R, Berta G, Ernszt D, Najbauer J, Németh P, Boldizsár F and Berki T. Glucocorticoid hormone treatment enhances the cytokine production of regulatory T cells by upregulation of Foxp3 expression. Immunobiology 2018; 223: 422-431.
[43] Lu Y, Zhang M, Wang S, Hong B, Wang Z, Li H, Zheng Y, Yang J, Davis RE, Qian J, Hou J and Yi Q. p38 MAPK-inhibited dendritic cells induce superior antitumour immune responses and overcome regulatory T-cell-mediated immunosuppression. Nat Commun 2014; 5: 4229.

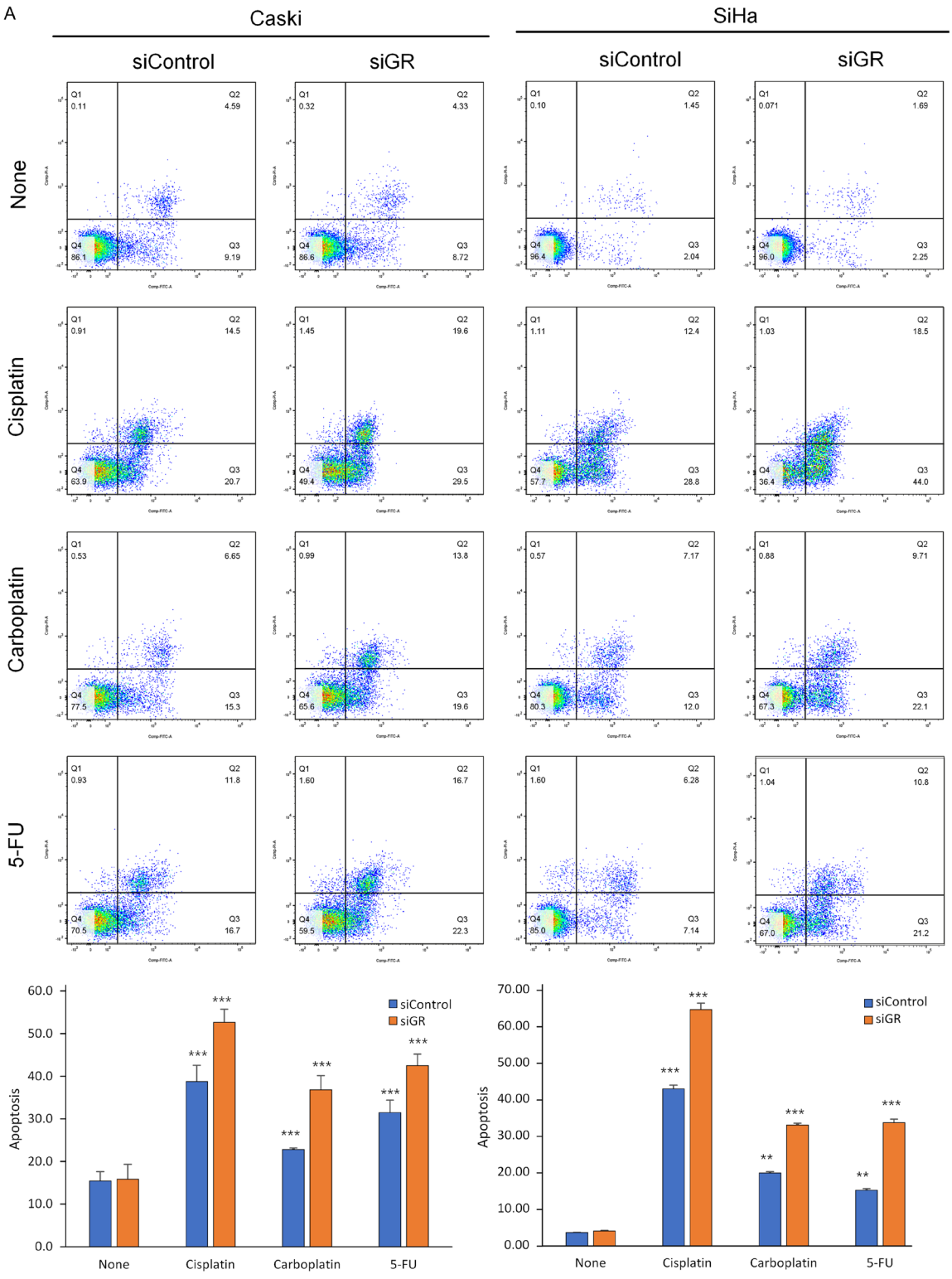
A
Caski
SiHa
siControl
siGR
siControl
siGR
None
Cisplatin
Carboplatin
5-FU
Q1 0.11
Q2 4.59
Q4 86.1
Q3 9.19
Q1 0.32
Q2 4.33
Q4 86.6
Q3 8.72
Q1 0.10
Q2 1.45
Q4 96.4
Q3 2.04
Q1 0.071
Q2 1.69
Q4 96.0
Q3 2.25
Q1 0.91
Q2 14.5
Q4 63.9
Q3 20.7
Q1 1.45
Q2 19.6
Q4 49.4
Q3 29.5
Q1 1.11
Q2 12.4
Q4 57.7
Q3 28.8
Q1 1.03
Q2 18.5
Q4 36.4
Q3 44.0
Q1 0.53
Q2 6.65
Q4 77.5
Q3 15.3
Q1 0.99
Q2 13.8
Q4 65.6
Q3 19.6
Q1 0.57
Q2 7.17
Q4 80.3
Q3 12.0
Q1 0.88
Q2 9.71
Q4 67.3
Q3 22.1
Q1 0.93
Q2 11.8
Q4 70.5
Q3 16.7
Q1 1.60
Q2 16.7
Q4 59.5
Q3 22.3
Q1 1.60
Q2 6.28
Q4 85.0
Q3 7.14
Q1 1.04
Q2 10.8
Q4 67.0
Q3 21.2
Apoptosis
60.0
50.0
40.0
30.0
20.0
10.0
0.0
siControl
siGR
None
Cisplatin
Carboplatin
5-FU
Apoptosis
70.00
60.00
50.00
40.00
30.00
20.00
10.00
0.00
siControl
siGR
None
Cisplatin
Carboplatin
5-FU

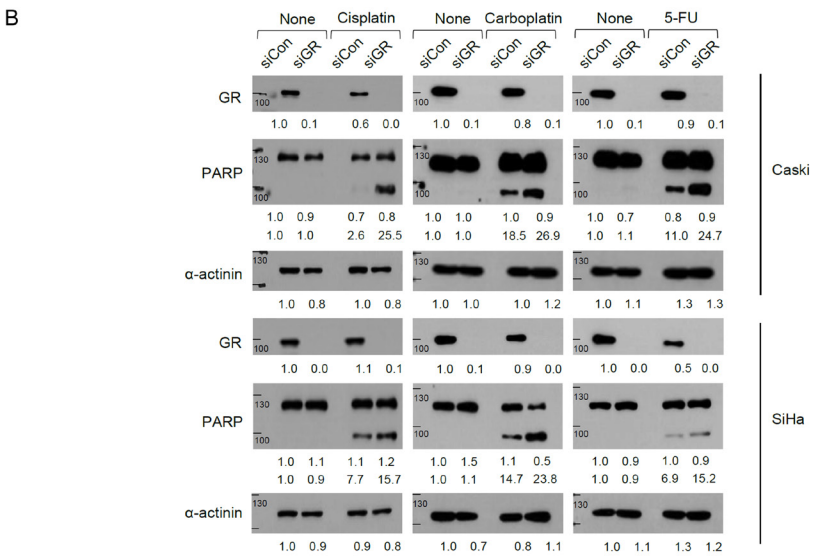

Supplementary Figure 1. A. Caski and SiHa cells were transfected with siRNA against GR for 48 hr followed by treatment with 20 μM cisplatin, 500 μM carboplatin, and 1 mM 5-fluorouracil for 24 hr. Cells were harvested and apoptosis was analyzed using flow cytometry after staining with annexin V-FITC/propidium iodide. Upper panel: representative scatter plots of propidium iodide (y-axis) versus annexin V (x-axis). Lower panel: Quantitative analysis of apoptotic cells. B. Protein expression of GR, PARP, and α-actinin was analyzed by western blotting (numbers below each blot are densitometric values).

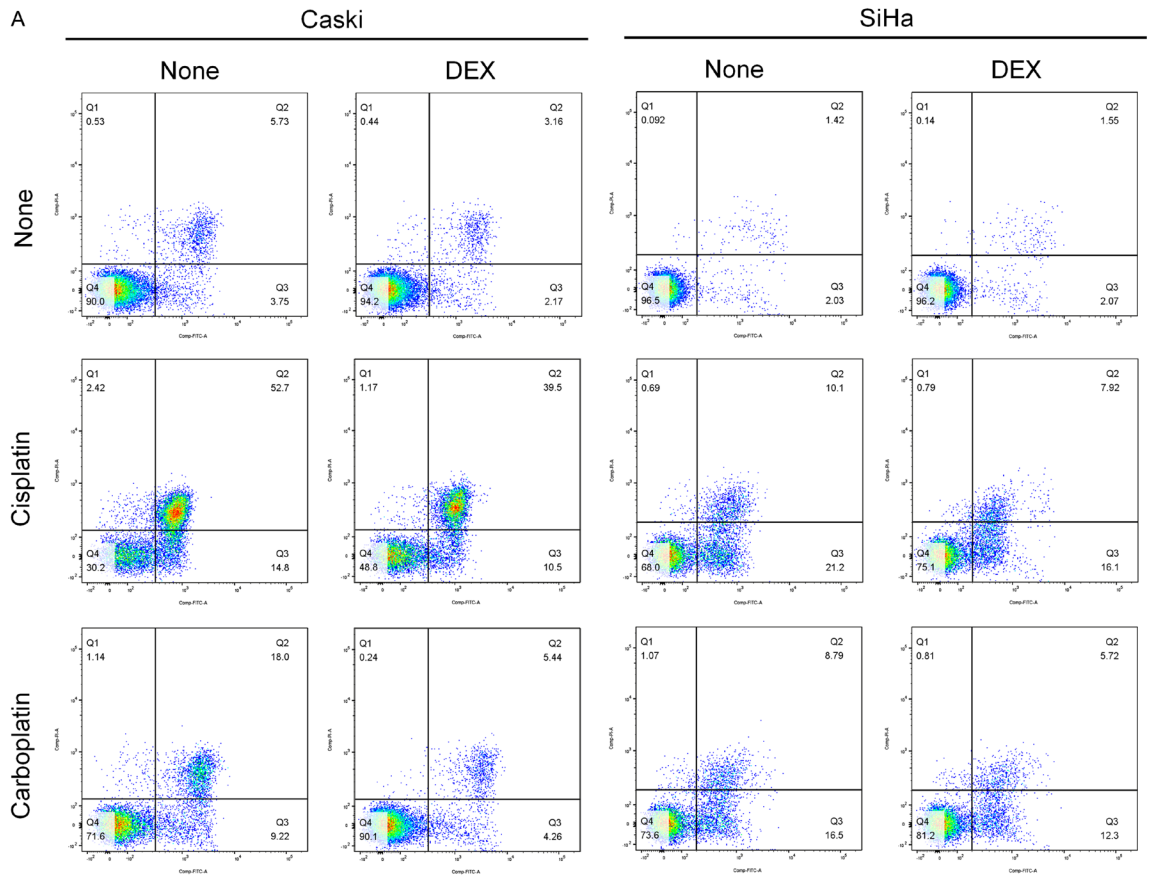

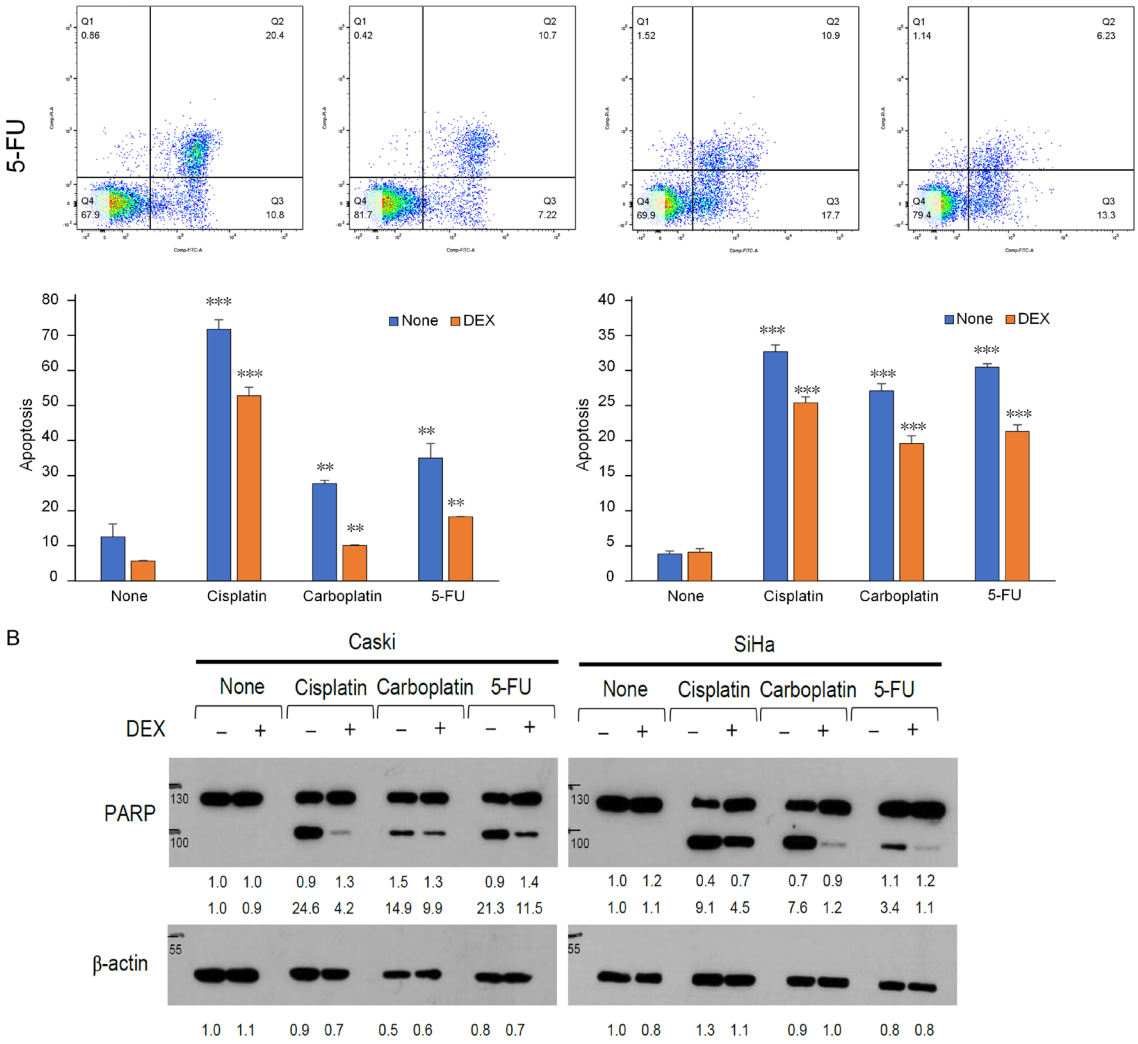

Supplementary Figure 2. A. Caski and SiHa cells were pre-treated with 1 μM dexamethsone for 3 hr followed by treatment with 20 μM cisplatin, 500 μM carboplatin, and 1 mM 5-fluorouracil for 48 hr. Cells were harvested and apoptosis was analyzed using flow cytometry after staining with annexin V-FITC/propidium iodide. Upper panel: representative scatter plots of propidium iodide (y-axis) versus annexin V (x-axis). Lower panel: Quantitative analysis of apoptotic cells. B. Protein expression of PARP and β-actin was analyzed by western blotting (numbers below each blot are densitometric values). The number of asterisks (*) indicates the level of significance: **P < 0.05, ***P < 0.005. Error bars represent mean ± standard error of triplicate experiments.

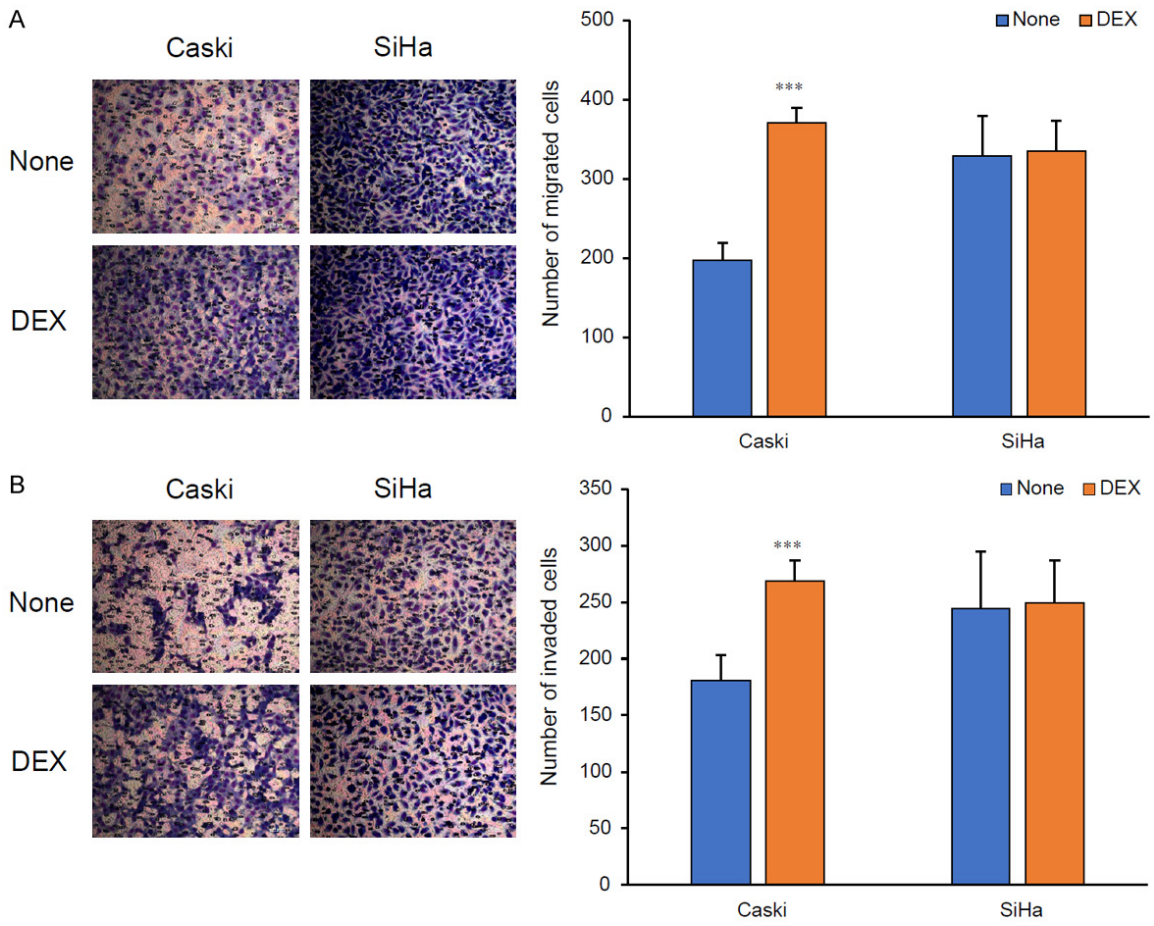

Supplementary Figure 3. Caski and SiHa cells were treated with 0.5 μM dexamethasone for 24 hr. A, B. Cell migration and invasion assays were conducted using the Boyden chamber assay. Left panel: representative image of the Boyden chamber assay (Scale bar 50 μM); Right panel: Quantitative result of the Boyden chamber assay.